EVOLUTIONARY BIOLOGY

Nuclear DNA from two early Neandertals reveals 80,000 years of genetic continuity in Europe

Stéphane Peyrégne[1]*, Viviane Slon[1], Fabrizio Mafessoni[1], Cesare de Filippo[1], Mateja Hajdinjak[1], Sarah Nagel[1], Birgit Nickel[1], Elena Essel[1], Adeline Le Cabec[2], Kurt Wehrberger[3], Nicholas J. Conard[4], Claus Joachim Kind[5], Cosimo Posth[6], Johannes Krause[6], Grégory Abrams[7], Dominique Bonjean[7], Kévin Di Modica[7], Michel Toussaint[8], Janet Kelso[1], Matthias Meyer[1], Svante Pääbo[1], Kay Prüfer[1,6]*

Little is known about the population history of Neandertals over the hundreds of thousands of years of their existence. We retrieved nuclear genomic sequences from two Neandertals, one from Hohlenstein-Stadel Cave in Germany and the other from Scladina Cave in Belgium, who lived around 120,000 years ago. Despite the deeply divergent mitochondrial lineage present in the former individual, both Neandertals are genetically closer to later Neandertals from Europe than to a roughly contemporaneous individual from Siberia. That the Hohlenstein-Stadel and Scladina individuals lived around the time of their most recent common ancestor with later Neandertals suggests that all later Neandertals trace at least part of their ancestry back to these early European Neandertals.

INTRODUCTION

Neandertals lived in western Eurasia for hundreds of thousands of years before modern humans spread outside Africa. The earliest morphological and genetic evidence of Neandertals reaches back approximately 430 thousand years (ka) ago (*1*, *2*), while the last Neandertals disappeared around 40 ka ago (*3*). Denisovans, a sister group of Neandertals discovered by genetic analysis of remains from Denisova Cave (Altai Mountains, Russia; Fig. 1) (*4*), may have been widespread in Asia (*5*).

Recent analyses of nuclear genome sequences from Neandertals have shown that, toward the end of their existence, Neandertals across their entire geographic range from Europe to Central Asia belonged to a single group sharing a most recent common ancestor less than 97 ka ago (*6*, *7*). However, population discontinuity has been observed in Denisova Cave, Russia, further back in time, where the Neandertal component in the genome of a ~90-ka-old Neandertal-Denisovan offspring (*7*) shows stronger affinities to late Neandertals in Europe than to the *Altai Neandertal*, another individual found in the same cave (*8*). The latter lived 120 ka ago according to the number of missing mutations in her genome compared to present-day human genomes. Thus, a population replacement likely occurred in the easternmost part of the Neandertal territory between 90 and 120 ka ago.

Without nuclear genome sequences from early European Neandertals, it has not been possible to determine the origin of the replacement and whether it was limited to the east. To learn more about the early population history of European Neandertals, we studied the nuclear genomes of two individuals from Western Europe that are dated to approximately 120 ka ago and from which only mitochondrial DNA (mtDNA) was previously recovered. The first, a femur from Hohlenstein-Stadel Cave (*HST*) in Germany (*9*), carries an mtDNA genome that falls basal to all other known Neandertal mtDNAs and was dated to ~124 ka ago based on its branch length in the mitochondrial tree [95% highest posterior density interval (HPDI), 62 to 183 ka ago; associated faunal remains suggest a date between 80 and 115 ka ago] (*10*). The second, a maxillary bone from Scladina Cave [*Scladina I-4A*, here referred to as *Scladina* (*11*)], yielded the hypervariable region of the mtDNA genome (*12*) and was dated to 127 ka ago based on uranium and thorium isotopic ratios [1 SD, 95 to 173 ka ago (*13*)].

RESULTS

Because of the great age of the specimens and their extensive handling in the decades after their discovery, obtaining DNA of sufficient quantity for genome-wide analyses is challenging. We thus used the most efficient DNA extraction and library preparation methods currently available (*14*–*16*) and coupled them with pretreatment methods for the removal of human and microbial contamination (note S1) (*17*). We then characterized the libraries prepared from both specimens by hybridization capture of mtDNA and shallow shotgun sequencing to identify those libraries that were most suitable for further analysis (Materials and Methods; notes S2 and S3). On the basis of 450- and 107-fold coverage of the mtDNA genome, respectively, we were able to verify the published mtDNA sequence from *HST* (*10*) and reconstruct the complete mtDNA of *Scladina* (notes S5 and S6). *Scladina* dates to ~120 ka ago according to the branch length in the mtDNA tree (95% HPDI, 76 to 168 ka ago; note S7), consistent with the aforementioned date. Confirming previous results from the hypervariable region (*10*), we find that the complete *Scladina* mtDNA is most similar to the *Altai Neandertal* mtDNA (note S7). On the basis of only the mtDNA, it thus appears that both individuals fall outside the variation of later European Neandertals. However, mtDNA is only a single maternally inherited locus and of limited value for reconstructing the relationships among Neandertals and other archaic humans (*1*).

[1]Department of Evolutionary Genetics, Max Planck Institute for Evolutionary Anthropology, Deutscher Platz 6, Leipzig04103, Germany. [2]Department of Human Evolution, Max Planck Institute for Evolutionary Anthropology, Deutscher Platz 6, Leipzig04103, Germany. [3]Museum Ulm, Marktplatz 9, Ulm89073, Germany. [4]Department of Early Prehistory and Quaternary Ecology, University of Tübingen, Schloss Hohentübingen, Tübingen72070, Germany. [5]State Office for Cultural Heritage Baden-Württemberg Berliner Strasse 12, Esslingen 73728 Germany. [6]Max Planck Institute for the Science of Human History, Khalaische Strasse 10, Jena07745, Germany. [7]Scladina Cave Archaeological Center, Sclayn, Belgium. [8]Ouffet, Belgium.
*Corresponding author. Email: stephane_peyregne@eva.mpg.de (S.Pe.); pruefer@eva.mpg.de (K.P.)

Fig. 1. Sites from which partial to complete nuclear genomes from Neandertals (or their ancestors in Sima de los Huesos) were retrieved. References (*1*, *6*, *8*, *20*, *34*–*36*) describe Neandertal genomic data from these sites. The origins of the two Neandertals studied here are highlighted in purple and blue, respectively.

We generated a total of 168 and 78 million base pairs (Mbp) of nuclear DNA sequence from the two individuals, respectively (note S3). Ancient DNA sequences often carry cytosine to thymine substitutions that are caused by cytosine deamination accumulating in DNA fragments over time, most often at the ends of the fragments (*18*). The frequency of these substitutions on both molecule ends (*1*), confirms that ancient nuclear DNA is present but that a large proportion of the *HST* and *Scladina* sequences are contaminants from present-day humans (note S8). At positions that are derived only in the *Altai Neandertal* [ancestral in the genomes of a Denisovan (*19*) and an Mbuti (*19*)], 57.8 and 31.1% of *HST* and *Scladina* sequences, respectively, show the Neandertal allele (note S9). However, sequences also match the derived allele in an Mbuti genome (*19*) more often than the high-coverage genome of the *Altai Neandertal* does (*HST*, 8.8%; *Scladina*, 22.3%, *Altai Neandertal*, 1.4%; note S8). This excess of sharing suggests that 23 and 65% of the *HST* and *Scladina* sequences, respectively, are modern human contaminants (note S8). To reduce contamination, we restricted all further analyses to sequences that show evidence for deamination (Materials and Methods), leaving us with 51 Mbp of the *HST* genome and 12 Mbp of the *Scladina* genome (note S3). This procedure reduces the estimated contamination to 2% for *HST* and 5.5% for *Scladina* and results in a coverage on the X chromosome and autosomes that shows that *HST* was male, whereas *Scladina* was female, in agreement with the morphological assessments (notes S4 and S8) (*9*, *13*).

To investigate the relationship of *HST* and *Scladina* to Neandertals, we compared their nuclear sequences to two high-coverage Neandertal genomes. The genome of a ~50-ka-old Neandertal from Vindija Cave in Croatia [*Vindija 33.19*, referred to as *Vindija* (*20*)] is a representative of the group of later Neandertals that inhabited Eurasia after 90 ka ago (*6*, *7*), whereas the *Altai Neandertal* represents the earlier group of Neandertals in the east. We identified Vindija-specific– and Altai-specific–derived variants by randomly sampling an allele from these two Neandertal genomes and retaining only those variants that differ from the other high-coverage Neandertal genome and from the Denisovan (*19*), one Mbuti (*19*), and several ape outgroup genomes (Materials and Methods) (*21*–*24*). At these sites, *HST* shares Vindija-specific alleles more often than Altai-specific alleles (531 versus 466; two-sided binomial test, $P = 0.043$), while no significant difference was observed for *Scladina* (110 versus 106; $P = 0.838$; Fig. 2 and note S9). Since the number of DNA sequences with putative deamination-induced substitutions is small for *Scladina*, we repeated this analysis including all sequences and found that *Scladina* then shows more Vindija-specific alleles than Altai-specific alleles (*Scladina*, 443 versus 321; $P < 10^{-4}$; *HST*, 1676 versus 1326; $P < 10^{-9}$; note S9). This cannot be accounted for by contamination with present-day human DNA, since the proportion of Neandertal ancestry in present-day humans is, on average, smaller than 3% (note S9). Thus, these results indicate that both *HST* and *Scladina* are more closely related to *Vindija* than they are to the *Altai Neandertal*.

If *HST* and *Scladina* truly have a most recent common ancestor with *Vindija* more recently than with the *Altai Neandertal*, then their genomes are expected to share derived alleles with the *Altai Neandertal* genome as often as the *Vindija* genome does. However, the genomes of *Vindija* and the *Altai Neandertal* share more derived alleles with each other than the *HST* or *Scladina* genomes share with either of them (Fig. 2 and note S9). This imbalance in allele sharing can largely be accounted for by a reference bias that favors the alignment of *HST* and *Scladina* sequences that carry a modern human reference allele over those carrying a Neandertal allele (note S9). By aligning to an alternative reference genome containing alleles seen in the high-coverage Neandertals, we recover further sequences that we combine with the original set of alignments and compensate for this bias (Fig. 2, Materials and Methods, and note S9). The remaining imbalance in allele sharing can be explained by contamination and sequencing errors in *Scladina* and *HST* (Fig. 2 and note S9).

Using the reference bias–corrected alignments and two methods, we estimated split times between the populations represented by *HST* and *Scladina* and the Vindija population (note S10). Our first estimates are based on the sharing of derived alleles by *HST*/*Scladina* at sites where the high-coverage *Vindija* genome is heterozygous [F(A|B) statistic (*8*, *20*)]. The estimated split times of *HST* and *Scladina* from the ancestor with *Vindija* are 101 ka ago [confidence interval (CI), 80 to 123 ka ago] and 100 ka ago (CI, 66 to 153 ka ago), respectively. The second estimates are based on a coalescent divergence

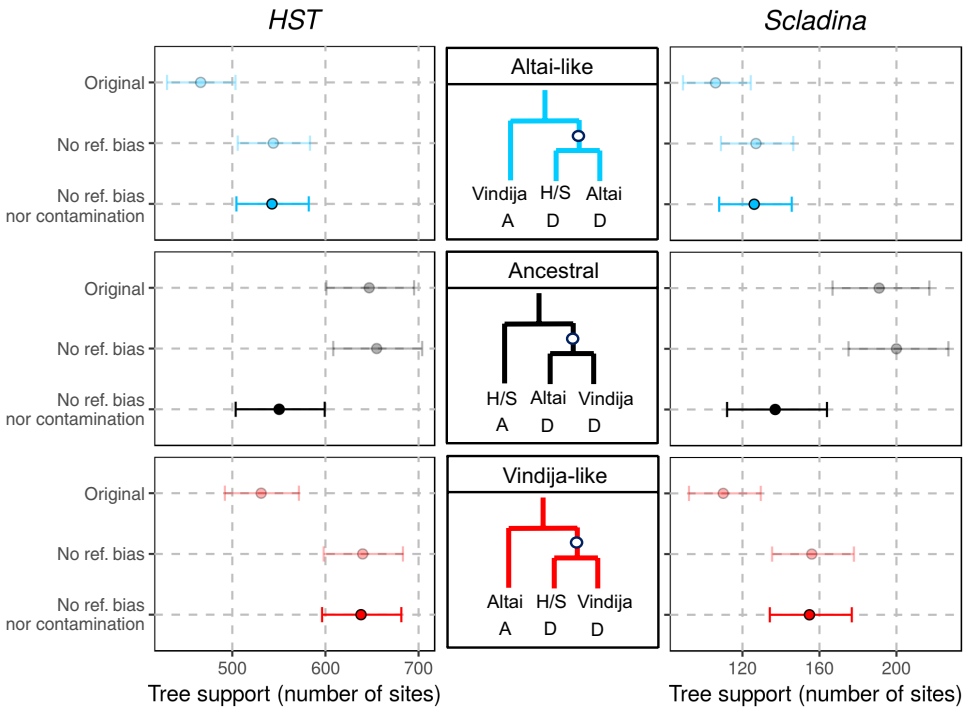

Fig. 2. Genetic relationship of *HST* and *Scladina* to *Vindija 33.19* and the Altai Neandertal. The three possible tree topologies relating these Neandertals (H/S, *HST* or *Scladina*) are depicted in the middle. Mutations occurring on the internal branch (white points) produce an allelic configuration (A, ancestral; D, derived) that is informative of the underlying tree topology. Genome-wide counts of sites with the described configurations are presented on both sides (*HST* on left and *Scladina* on right) on the *x* axis. Lighter colors correspond to results using the alignments to the human reference hg19 (original) and to both hg19 and the Neandertalized reference (no reference bias). The darker points are corrected for present-day human DNA contamination assuming 2.0 and 5.5% contamination in the deamination-filtered fragments from *HST* and *Scladina*, respectively. The Vindija-like configuration (red) is the most supported topology after correcting for reference bias and contamination. The two other topologies are the result of incomplete lineage sorting and are equally likely. Bars represent 95% binomial CIs.

model (*25*) and suggest, for both Neandertals, a ~10-ka-long shared history with *Vindija* after the split of the latter from the *Altai Neandertal* population (i.e., 122 to 141 ka ago, assuming 130 to 145 ka ago for the Vindija-Altai split time; note S10). The estimates from both methods are close to the estimated age of ~120 ka ago for these individuals (*10*, *13*). Therefore, *HST* and *Scladina* could be members of an ancestral Neandertal population that gave rise to all Neandertals sequenced to date with the exception of the *Altai Neandertal*, who did not leave any descendants among sequenced Neandertals. This ancestral Neandertal population was established in the west by ~120 ka ago, and later descendants may have migrated east and replaced at least partially the eastern population of Neandertals represented by the *Altai Neandertal*.

It seems unexpected that *HST* carries an mtDNA lineage that diverged ~270 ka ago from other mtDNAs, given the recent population split times from the *Vindija* ancestors and the low levels of genetic diversity in the nuclear genomes of Neandertals (*8*, *20*). To test whether such a deeply diverging mtDNA lineage could be maintained in the Neandertal population by chance, we used coalescent simulations with a demography estimated from the high-coverage Neandertal genomes (*20*), which was scaled to match the lower effective population size of the mtDNA, taking into account the difference in effective population size between the two sexes (*8*). We find that population split times between *HST* and other Neandertals of less than 150 ka ago make the occurrence of a mitochondrial time to the most recent common ancestor (TMRCA) of 270 ka ago unlikely (1.2% of all simulated loci have such a deep TMRCA; note S11). We note that this result is robust to uncertainties in the estimates of the Neandertal population size and of the mitochondrial TMRCA (note S11). The presence of this deeply divergent mtDNA in *HST* thus suggests a more complex scenario in which *HST* carries some ancestry from a genetically distant population.

DISCUSSION

What scenarios could explain the deeply divergent mtDNA in *HST*? An explanation could be related to a replacement of mtDNAs in Neandertals that has been suggested to explain the discrepancy between the mtDNA divergence time (<470 ka ago) (*10*) and the population split times based on nuclear DNA (>520 ka ago) (*20*) between modern humans and Neandertals. The Sima de los Huesos hominins, and perhaps other early Neandertals, carried mtDNAs that shared a common ancestor with Denisovan mtDNAs more recently than with those of modern humans, whereas later Neandertals carried mtDNAs that shared a more recent common ancestor with the mtDNAs of modern humans. Admixture between Neandertals and ancestors or relatives of modern humans could explain the origin of this later Neandertal mtDNA (*1*, *10*). If several mtDNAs were introduced into the Neandertal population by such a putative gene flow, then the deeply divergent mtDNA in *HST* may represent the remnants of the mitochondrial diversity of this introgressing population (Fig. 3) (*10*). This would imply that this admixture into Neandertals occurred later than the previously suggested lower boundary of 270 ka ago (219 to 316 ka ago) (*10*). We estimate that

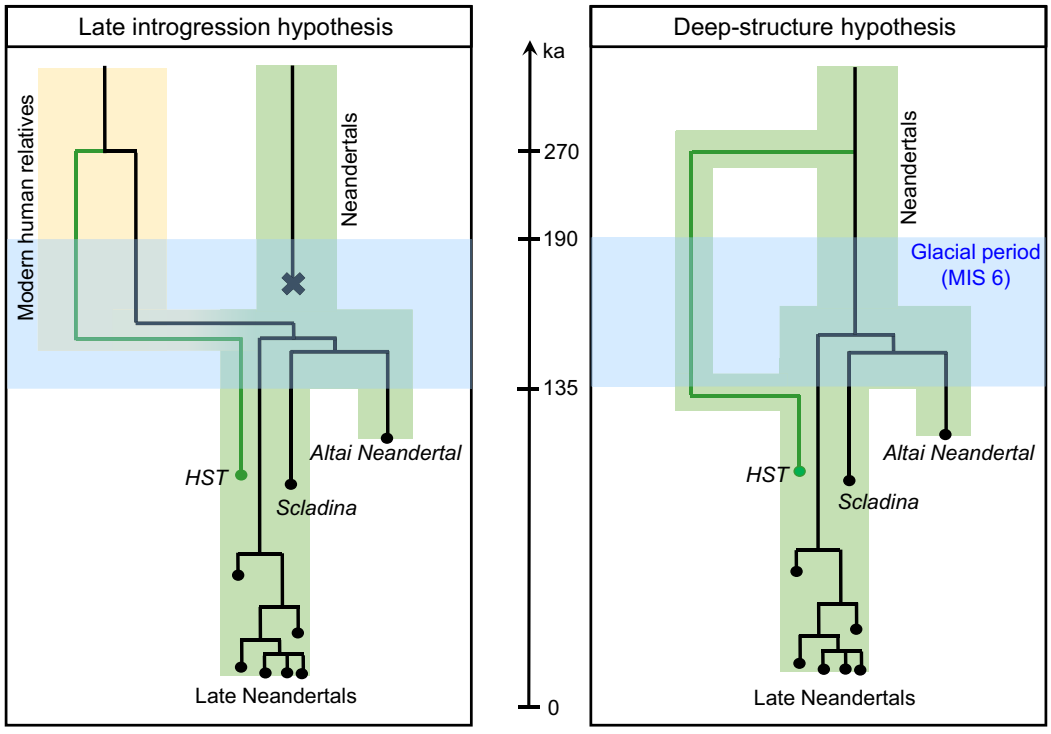

Fig. 3. Two scenarios to explain the deep divergence of *HST's* mtDNA to other Neandertal mtDNAs. The *HST* mitochondrial lineage is shown as a green line; all other Neandertal mtDNAs are shown in black. Green and yellow areas indicate populations (Neandertals in green and relatives of modern humans in yellow). The area shaded in blue shows the glacial period (MIS 6, marine isotope stage 6) (*37*). Note that all Neandertal mtDNA lineages in the right-hand scenario could be introgressed from modern human relatives before 270 ka ago (*10*).

the probability for this late mtDNA replacement is nearly identical to the admixture rate, i.e., more than 5% admixture is required to reach a probability of 5% for such an event to occur (note S12) (*10*).

An alternative source for the deeply divergent mtDNA in *HST* could be an isolated Neandertal population, for example, a population that separated from other Neandertals before the glacial period preceding *HST* and *Scladina* (~130 to 190 ka ago; Fig. 3). Such an isolated population may have preserved the mtDNA that was later re-introduced during a warmer period between 115 and 130 ka ago (the "Eemian" period) when these populations met again and gene flow resumed. We note that the contact may have been a result of a recolonization from the Middle East or Southern Europe (*26*, *27*).

Our analysis shows that late Neandertals that lived in Europe at around 40 ka ago trace at least part of their ancestry back to Neandertals that lived there approximately 80,000 years earlier. The latter became widespread, appearing in the east at least 90 ka ago. The genetic continuity seen in Europe contrasts, however, with the deeply divergent mtDNA in *HST*, which hints at a more complex history that affected at least some of the European Neandertals before ~120 ka ago. DNA sequences from even older Neandertals are needed to clarify whether Neandertal substructure, gene flow from relatives of modern humans, or both are the explanation for *HST's* peculiar mtDNA.

MATERIALS AND METHODS

DNA extraction and library preparation

Bone or tooth powder was sampled from the *HST* and *Scladina* specimens using a sterile dentistry drill after removing the external surface of the specimen at the sampling site (note S1). For the initial assessment of ancient DNA preservation in the specimens, DNA was extracted using a silica-based method (*14*), as implemented in (*17*), either from untreated powder or following one of three decontamination procedures described in the note S1. The treatment of the bone powder with 0.5% sodium hypochlorite yielded the highest proportion of fragments mapping to the human reference genome for *HST* and resulted in the lowest estimates of contamination by present-day human mtDNA for both *HST* and *Scladina* (note S2). For the subsequent generation of additional sequencing data, the bone or tooth powder was therefore incubated in 0.5% sodium hypochlorite solution before DNA extraction (*17*). Single-stranded DNA libraries were prepared from these DNA extracts (*15*, *16*). Each library was tagged with two unique indexes, amplified into plateau, and purified (*17*, *28*) before shotgun sequencing. In addition, an aliquot of each indexed DNA library was enriched for human mtDNA fragments using a hybridization capture method (*29*).

Sequencing and raw data processing

Libraries were sequenced on an Illumina MiSeq and HiSeq 2500 platforms in 76-cycle paired-end runs (*28*). For a detailed description of the read processing, see note S3. When analyzing the relationship of *HST* and *Scladina* to *Vindija* and the *Altai Neandertal*, further processing was necessary to avoid a reference bias of the alignments. First, we aligned DNA sequences to both the human reference genome (GRCh37/hg19) and a modified ("Neandertalized") version of the reference genome that includes the alternative alleles seen in *Vindija* and/or the *Altai Neandertal*. If there was more than one alternative base at a given site (i.e., a triallelic site), then a random

base was chosen. We then merged sequences that aligned to either reference genome and removed one duplicate of the sequences that mapped to both. If a sequence aligned to the two references at different positions, then both alignments were excluded (representing 522 and 332 such sequences for *HST* and *Scladina*, respectively). We developed an algorithm called bam-mergeRef to perform these merging steps, wrote it in C++, and made it available on GitHub (https://github.com/StephanePeyregne/bam-mergeRef). For a description of the reference bias and the effects of this processing, see note S9. Sequences from libraries enriched for mtDNA fragments were aligned to the revised Cambridge reference sequence (*30*) or the *Altai Neandertal* mtDNA with the same parameters as those applied to nuclear sequences (note S3).

Analysis of the mitochondrial genomes

Mitochondrial genome sequences were reconstructed from a consensus call at each position where at least two-thirds of the fragments aligning to the *Altai Neandertal* mtDNA carried the same base and if the position was covered by at least three fragments. Further details about the mtDNA reconstruction and the estimated proportion of contamination by present-day human mtDNA for both specimens, as well as the phylogenetic analyses, are described in notes S5 to S7.

Analysis of the relationship to other archaic and modern humans

We determined lineage-specific derived alleles by comparing the high-quality genomes of *Vindija* and the *Altai Neandertal* (*8*, *20*), *Denisova 3* (*19*), and a present-day human from Africa [Mbuti, HGDP00456 (*19*)]. At sites where one of these individuals was heterozygous, we randomly picked an allele. An allele was regarded as ancestral when it matched at least three of four aligned great ape reference genome assemblies [chimpanzee (panTro4) (*21*), bonobo (panPan1.1) (*22*), gorilla (gorGor3) (*23*), and orangutan (ponAbe2) (*24*); LASTZ alignments to the human genome GRCh37/hg19 prepared in-house and by the University of California, Santa Cruz, genome browser (*31*)]. The fourth ape was allowed to carry a third allele or have missing data but not to carry the alternative allele. To avoid errors from ancient DNA damage on *HST* and *Scladina* sequences at these positions, we only considered sequences that aligned in forward orientation when the ancestral or derived allele at the position was a G or in reverse orientation when either allele was a C and excluded sequences with a third allele. Only positions passing the published map35_100 filter for *Denisova 3*, *Vindija*, and the *Altai Neandertal* genotypes (*20*) were retained. A correction for the level of present-day human DNA contamination was applied in this analysis and is described in note S9.

Assessment of present-day human nuclear DNA contamination

We estimated contamination from the proportion p of sites where the Neandertal (*HST* or *Scladina*) carries a derived allele seen in the genome of a present-day Mbuti individual [HGDP00456 (*19*)] but not in *Denisova 3* and a Neandertal high-coverage genome (either *Vindija* or the *Altai Neandertal*). This proportion p is the result of a mixture of present-day human DNA contamination and DNA endogenous to the ancient specimens as follows: $c \times p_c + (1 - c) \times p_e = p$, with p_c and p_e being the expected proportions of derived alleles for the contaminant and endogenous molecules, respectively, and c is the contamination rate. The proportions p_c and p_e are unknown but can be approximated by the observed proportion of shared alleles between the Mbuti genome and another present-day human genome [33.2% for either a French, HGDP00521 (*19*) or a Han, HGDP00775 (*8*)] or a Neandertal high-coverage genome (1.4% for the *Altai Neandertal* and 1.5% for *Vindija*), respectively. To compute p_c and p_e, we used the genotypes from the high-coverage genomes (randomly sampling one allele at heterozygous positions) under the assumption that these are unaffected by sequencing errors or present-day human DNA contamination. CIs were calculated from the bounds of the binomial CIs of p. Assuming that p is the parameter of a binomial distribution (instead of the expected success rate in Poisson trials) is a conservative approximation for calculating CIs, as the variance for Poisson trials is lower or equal to the variance of the binomial distribution with parameter p.

Coalescent simulations of the mitochondrial common ancestor

Coalescent simulations using scrm (*32*) were used to compute the expected distribution of times to TMRCAs for the mitochondrial genomes, given different population split times (from 100 to 200 ka ago, with a step of 10 ka). To be able to compare these to the estimated date for the common mitochondrial ancestor of *HST* and *Vindija*, the simulations followed the *Vindija* demographic history estimated from the Pairwise Sequentially Markovian Coalescent model (PSMC) (*33*) [that assumed a mutation rate of 1.45×10^{-8} per base pair per generation and a generation time of 29 years (*20*)]. The scaling for the mitochondrial effective population size was calculated according to the females-to-males ratio, previously estimated to be 1.54 for the Altai Neandertal population (note S11) (*8*).

SUPPLEMENTARY MATERIALS

Supplementary material for this article is available at http://advances.sciencemag.org/cgi/content/full/5/6/eaaw5873/DC1

Note S1. Ancient DNA recovery and treatment.
Note S2. Decontamination methods and initial screening.
Note S3. Data generation and data processing.
Note S4. Sex determination.
Note S5. Mitochondrial contamination estimates.
Note S6. Reconstruction of the mitochondrial genomes.
Note S7. Phylogenetic analysis of the mitochondrial genomes.
Note S8. Characterization of present-day human DNA contamination in the nuclear genome.
Note S9. Genetic relationships and effect of present-day human DNA contamination, sequencing errors, and reference bias.
Note S10. Split time estimates.
Note S11. Discordance between the nuclear and mitochondrial divergence of *HST* to other Neandertals.
Note S12. Likelihood of a recent mitochondrial replacement in Neandertals.
Table S1. Overview of DNA extracts and libraries prepared from the *HST* femur.
Table S2. Overview of DNA extracts and libraries prepared for *Scladina I-4A*.
Table S3. DNA content in the libraries prepared from *HST* extracts prepared following different decontamination methods (set 1 in table S1).
Table S4. DNA content in the libraries prepared from the bone powder treated with sodium hypochlorite.
Table S5. DNA content in the initial libraries prepared from the untreated extracts from *Scladina I-4A*.
Table S6. Present-day human DNA contamination estimates after three decontamination methods applied to bone powder from the *HST* femur.
Table S7. Present-day human DNA contamination estimates from *Scladina I-4A* mtDNA based on differences between Neandertals and modern humans.
Table S8. Sequencing summary statistics for *HST* with the following filters: length (≥35 bp) and mapping quality (≥25).
Table S9. Sequencing summary statistics for *HST* with the following filters: length (≥30 bp) and mapping quality (≥25).

Table S10. Sequencing summary statistics for *Scladina I-4A* with the following filters: length (≥35 bp) and mapping quality (≥25).
Table S11. Sequencing summary statistics for *Scladina I-4A* with the following filters: length (≥30 bp) and mapping quality (≥25).
Table S12. Sequencing statistics of the negative controls for *HST* (see table S1).
Table S13. Sequencing statistics of the negative controls for *Scladina I-4A* (see table S2).
Table S14. Summary of *HST* mtDNA sequencing.
Table S15. Summary of *Scladina I-4A* mtDNA sequencing.
Table S16. Coverage statistics for all sequences from *HST* within the alignability track, map35_L100.
Table S17. Coverage statistics for *HST* sequences with a C-to-T substitution within the three first or last positions of either ends.
Table S18. Coverage statistics for all sequences from *Scladina I-4A* within the alignability track, map35_L100.
Table S19. Coverage statistics for *Scladina I-4A* sequences with a C-to-T substitution within the three first or last positions of either ends.
Table S20. Present-day human DNA contamination estimates from *HST* mtDNA.
Table S21. Present-day human DNA contamination estimates from *Scladina I-4A* mtDNA based on differences between Neandertals and modern humans.
Table S22. Present-day human DNA contamination estimates from *Scladina I-4A* mtDNA based on differences between *Scladina I-4A* and modern humans.
Table S23. Present-day human DNA contamination estimates on mtDNA in the blank libraries of *HST* based on differences between *HST* and modern humans.
Table S24. Present-day human DNA contamination estimates on mtDNA in the blank libraries of *Scladina I-4A* based on differences between Neandertals and modern humans.
Table S25. Best substitution models according to the three model selection measures computed by jModelTest 2.1.10.
Table S26. Marginal likelihoods of the different tested clock and tree models obtained from a path sampling approach using only the coding region of the mitochondrial sequences.
Table S27. Marginal likelihoods of the different tested clock and tree models obtained from a path sampling approach using the full mitochondrial genome sequences.
Table S28. Estimates of molecular age and divergence times.
Table S29. Present-day human DNA contamination estimates for *HST* nuclear DNA based on deamination rates on the last positions of the molecules.
Table S30. Present-day human DNA contamination estimates for *Scladina I-4A* nuclear DNA based on deamination rates on the last positions of the molecules.
Table S31. Relationship between sequence length and present-day human DNA contamination estimate based on deamination rates in *HST* nuclear DNA sequences.
Table S32. Present-day human DNA contamination estimates based on the sharing of derived alleles with a modern human.
Table S33. Genome-wide counts of the three possible allelic configurations informative about the underlying topologies relating *Vindija 33.19* and the Altai Neandertal to *HST* and *Scladina I-4A* before correcting for reference bias or contamination (see tables S40 and S41 for corrected results and fig. S17 for a description of these allelic configurations).
Table S34. Comparison of alignments to hg19 and panTro4.
Table S35. Excess of ancestral alleles in Late Neandertals compared to *Vindija 33.19* at sites that are derived in the Altai Neandertal genome but ancestral in the genomes of an Mbuti and a Denisovan.
Table S36. Effect of the modified alignment procedure on the allele sharing with the Altai Neandertal.
Table S37. Alleles seen in *Vindija 87* at positions that are heterozygous in *Vindija 33.19*.
Table S38. Sequencing and alignment errors of *Vindija 87* sequences at positions where *Vindija 33.19* is homozygous different from the Altai Neandertal, comparing the original alignments to hg19 with our modified alignment procedure.
Table S39. Summary of the alignments to the two references.
Table S40. Applying different sequence lengths cutoffs does not affect the allele sharing with the Altai Neandertal after realignments.
Table S41. Genome-wide counts of the three possible allelic configurations informative about the underlying topologies relating *Vindija 33.19* and the Altai Neandertal to *HST* and *Scladina I-4A* after correcting for reference bias (see table S33 to compare with uncorrected results and table S42 for results corrected for contamination).
Table S42. Counts of the three possible allelic configurations informative about the underlying topologies relating *Vindija 33.19* and the Altai Neandertal to *HST* and *Scladina I-4A* after correcting for both reference bias and contamination.
Table S43. Summary statistics about the physical distance between the positions used to infer the genetic relationship of *HST* to *Vindija 33.19* and the Altai Neandertal.
Table S44. Summary statistics about the physical distance between the positions used to infer the genetic relationship of *Scladina I-4A* to *Vindija 33.19* and the Altai Neandertal.
Table S45. Effective number of independent positions.
Table S46. Comparison between split time estimates from the Vindija population based on a coalescent divergence model and the F(A|B) statistic for five low-coverage Neandertal genomes.
Table S47. Split time estimates from the Vindija population based on a coalescent divergence model.
Table S48. Age estimate for individual B (branch shortening) used to convert the F(A|B) values shown in table S47 into time before present.
Table S49. Summary of the number of sites and blocks used to compute the F(A|B) statistic and CIs.
Table S50. Split time estimates between *HST* or *Scladina I-4A* and different populations (population B) based on the calibration of the F(A|B) statistic.
Table S51. Predictions of the mitochondrial TMRCA given different split times between the populations of *HST* and *Vindija 33.19*.
Table S52. Predictions of the mitochondrial TMRCA given different split times between the *Vindija 33.19* population and a hypothetical isolated Neandertal population.
Table S53. Predictions of the mitochondrial TMRCA as done for table S51 but using either the upper or the lower estimates of the Neandertal population size.
Fig. S1. Length distribution of unique DNA fragments aligned to the human reference genome hg19 with a mapping quality of 25 or above (average length = 33 bp for *HST* and 25 bp for *Scladina I-4A*) and mapping uniquely (alignability track, map35_L100).
Fig. S2. Proportion of spurious alignment for different sequence lengths in the three libraries of *HST* that represent ~80% of the generated sequences for this specimen.
Fig. S3. Proportion of spurious alignment in the libraries of *Scladina I-4A* (same as for *HST* in fig. S2).
Fig. S4. Bivariate plot of root length against labio-lingual crown diameter (in millimeter) for the permanent mandibular canine.
Fig. S5. Bivariate plot of root length against labio-lingual crown diameter (in millimeter) for the permanent maxillary central incisor.
Fig. S6. Bivariate plot of root pulp volume against total root volume (in cubic millimeter) for the permanent maxillary central incisor.
Fig. S7. Ratio of sequences aligning to the X chromosome and autosomes.
Fig. S8. Number of sequences mapping to each chromosome normalized by chromosome length.
Fig. S9. Deamination patterns from the mtDNA.
Fig. S10. Maximum parsimony tree built with MEGA6 (Molecular Evolutionary Genetics Analysis, program version 6).
Fig. S11. Phylogenetic relationship of currently available archaic human mitochondrial genomes reconstructed from a Bayesian analysis with BEAST 2 (Bayesian Evolutionary Analysis Sampling Trees, program version 2).
Fig. S12. C-to-T substitution frequencies at the end of nuclear DNA sequences (dashed lines), including frequencies conditioned on a C-to-T substitution at the other end (solid lines).
Fig. S13. Proportion of alleles that are derived in the Altai Neandertal but ancestral in the *Vindija 33.19* Neandertal and Denisovan genomes stratified by the allele frequency in the Luhya and Yoruba populations (AFR) of the 1000 genomes dataset.
Fig. S14. Deamination frequencies on sequences from *HST* that carry a modern human allele absent from the currently available Neandertal genomes.
Fig. S15. Deamination frequencies on sequences from *Scladina I-4A* that carry a modern human allele absent from the currently available Neandertal genomes.
Fig. S16. Lineage assignment before correcting for the reference bias.
Fig. S17. Expectations for the genetic relationship of *HST* and *Scladina I-4A* to *Vindija 33.19* and the Altai Neandertal.
Fig. S18. Lineage assignment after correcting for the reference bias.
Fig. S19. Comparison of the expected and observed mitochondrial TMRCA of *HST* with other European Neandertals.
Fig. S20. Probability that all sampled Neandertal mtDNAs come from an early modern human population as a function of the admixture rate.
Fig. S21. Probability that all sampled Neandertal mtDNAs come from an early modern human population as a function of the admixture rate.
References (*38*–*114*)

REFERENCES AND NOTES

1. M. Meyer, J.-L. Arsuaga, C. de Filippo, S. Nagel, A. Aximu-Petri, B. Nickel, I. Martínez, A. Gracia, J. M. B. de Castro, E. Carbonell, B. Viola, J. Kelso, K. Prüfer, S. Pääbo, Nuclear DNA sequences from the Middle Pleistocene Sima de los Huesos hominins. *Nature* **531**, 504–507 (2016).
2. J. L. Arsuaga, I. Martínez, L. J. Arnold, A. Aranburu, A. Gracia-Téllez, W. D. Sharp, R. M. Quam, C. Falguères, A. Pantoja-Pérez, J. Bischoff, E. Poza-Rey, J. M. Parés, J. M. Carretero, M. Demuro, C. Lorenzo, N. Sala, M. Martinon-Torres, N. Garcia, A. Alcazar de Velasco, G. Cuenca-Bescós, A. Gómez-Olivencia, D. Moreno, A. Pablos, C. C. Shen, L. Rodríguez, A. I. Ortega, R. García, A. Bonmatí, J. M. Bermúdez de Castro, E. Carbonell, Neandertal roots: Cranial and chronological evidence from Sima de los Huesos. *Science* **344**, 1358–1363 (2014).
3. T. Higham, K. Douka, R. Wood, C. B. Ramsey, F. Brock, L. Basell, M. Camps, A. Arrizabalaga, J. Baena, C. Barroso-Ruíz, C. Bergman, C. Boitard, P. Boscato, M. Caparrós, N. J. Conard, C. Draily, A. Froment, B. Galván, P. Gambassini, A. Garcia-Moreno, S. Grimaldi, P. Haesaerts, B. Holt, M.-J. Iriarte-Chiapusso, A. Jelinek, J. F. Jordá Pardo, J.-M. Maíllo-Fernández, A. Marom, J. Maroto, M. Menéndez, L. Metz, E. Morin, A. Moroni, F. Negrino, E. Panagopoulou, M. Peresani, S. Pirson, M. de la Rasilla, J. Riel-Salvatore, A. Ronchitelli, D. Santamaria, P. Semal, L. Slimak, J. Soler, N. Soler, A. Villaluenga, R. Pinhasi, R. Jacobi,

The timing and spatiotemporal patterning of Neanderthal disappearance. *Nature* **512**, 306–309 (2014).
4. D. Reich, R. E. Green, M. Kircher, J. Krause, N. Patterson, E. Y. Durand, B. Viola, A. W. Briggs, U. Stenzel, P. L. F. Johnson, T. Maricic, J. M. Good, T. Marques-Bonet, C. Alkan, Q. Fu, S. Mallick, H. Li, M. Meyer, E. E. Eichler, M. Stoneking, M. Richards, S. Talamo, M. V. Shunkov, A. P. Derevianko, J.-J. Hublin, J. Kelso, M. Slatkin, S. Pääbo, Genetic history of an archaic hominin group from Denisova Cave in Siberia. *Nature* **468**, 1053–1060 (2010).
5. S. R. Browning, B. L. Browning, Y. Zhou, S. Tucci, J. M. Akey, Analysis of human sequence data reveals two pulses of archaic Denisovan admixture. *Cell* **173**, 53–61. e9 (2018).
6. M. Hajdinjak, Q. Fu, A. Hübner, M. Petr, F. Mafessoni, S. Grote, P. Skoglund, V. Narasimham, H. Rougier, I. Crevecoeur, P. Semal, M. Soressi, S. Talamo, J.-J. Hublin, I. Gušić, Ž. Kućan, P. Rudan, L. V. Golovanova, V. B. Doronichev, C. Posth, J. Krause, P. Korlević, S. Nagel, B. Nickel, M. Slatkin, N. Patterson, D. Reich, K. Prüfer, M. Meyer, S. Pääbo, J. Kelso, Reconstructing the genetic history of late Neanderthals. *Nature* **555**, 652–656 (2018).
7. V. Slon, F. Mafessoni, B. Vernot, C. de Filippo, S. Grote, B. Viola, M. Hajdinjak, S. Peyrégne, S. Nagel, S. Brown, K. Douka, T. Higham, M. B. Kozlikin, M. V. Shunkov, A. P. Derevianko, J. Kelso, M. Meyer, K. Prüfer, S. Pääbo, The genome of the offspring of a Neanderthal mother and a Denisovan father. *Nature* **561**, 113–116 (2018).
8. K. Prüfer, F. Racimo, N. Patterson, F. Jay, S. Sankararaman, S. Sawyer, A. Heinze, G. Renaud, P. H. Sudmant, C. de Filippo, H. Li, S. Mallick, M. Dannemann, Q. Fu, M. Kircher, M. Kuhlwilm, M. Lachmann, M. Meyer, M. Ongyerth, M. Siebauer, C. Theunert, A. Tandon, P. Moorjani, J. Pickrell, J. C. Mullikin, S. H. Vohr, R. E. Green, I. Hellmann, P. L. F. Johnson, H. Blanche, H. Cann, J. O. Kitzman, J. Shendure, E. E. Eichler, E. S. Lein, T. E. Bakken, L. V. Golovanova, V. B. Doronichev, M. V. Shunkov, A. P. Derevianko, B. Viola, M. Slatkin, D. Reich, J. Kelso, S. Pääbo, The complete genome sequence of a Neanderthal from the Altai Mountains. *Nature* **505**, 43–49 (2014).
9. M. Kunter, J. Wahl, Das Femurfragment eines Neandertalers aus der Stadelhöhle des Hohlensteins im Lonetal. *Fundberichte aus Baden-Württemberg* **17**, 111–124 (1992).
10. C. Posth, C. Wißing, K. Kitagawa, L. Pagani, L. van Holstein, F. Racimo, K. Wehrberger, N. J. Conard, C. J. Kind, H. Bocherens, J. Krause, Deeply divergent archaic mitochondrial genome provides lower time boundary for African gene flow into Neanderthals. *Nat. Commun.* **8**, 16046 (2017).
11. M. Toussaint, M. Otte, D. Bonjean, H. Bocherens, C. Falguères, Y. Yokoyama, Les restes humains néandertaliens immatures de la couche 4A de la grotte Scladina (Andenne, Belgique). *Comptes Rendus de l'Académie des Sciences-Series IIA-Earth and Planetary Science* **326**, 737–742 (1998).
12. L. Orlando, P. Darlu, M. Toussaint, D. Bonjean, M. Otte, C. Hänni, Revisiting Neandertal diversity with a 100,000 year old mtDNA sequence. *Curr. Biol.* **16**, R400–R402 (2006).
13. M. Toussaint, D. Bonjean, *The Scladina I-4A Juvenile Neandertal, Andenne, Belgium: Palaeoanthropology and Context* (ERAUL Editions, 2014).
14. J. Dabney, M. Knapp, I. Glocke, M.-T. Gansauge, A. Weihmann, B. Nickel, C. Valdiosera, N. García, S. Pääbo, J.-L. Arsuaga, M. Meyer, Complete mitochondrial genome sequence of a Middle Pleistocene cave bear reconstructed from ultrashort DNA fragments. *Proc. Natl. Acad. Sci. U. S. A.* **110**, 15758–15763 (2013).
15. M.-T. Gansauge, T. Gerber, I. Glocke, P. Korlević, L. Lippik, S. Nagel, L. M. Riehl, A. Schmidt, M. Meyer, Single-stranded DNA library preparation from highly degraded DNA using T4 DNA ligase. *Nucleic Acids Res.* **45**, e79 (2017).
16. M.-T. Gansauge, M. Meyer, Single-stranded DNA library preparation for the sequencing of ancient or damaged DNA. *Nat. Protoc.* **8**, 737–748 (2013).
17. P. Korlević, T. Gerber, M.-T. Gansauge, M. Hajdinjak, S. Nagel, A. Aximu-Petri, M. Meyer, Reducing microbial and human contamination in DNA extractions from ancient bones and teeth. *Biotechniques* **59**, 87–93 (2015).
18. A. W. Briggs, U. Stenzel, P. L. F. Johnson, R. E. Green, J. Kelso, K. Prüfer, M. Meyer, J. Krause, M. T. Ronan, M. Lachmann, S. Pääbo, Patterns of damage in genomic DNA sequences from a Neandertal. *Proc. Natl. Acad. Sci. U. S. A.* **104**, 14616–14621 (2007).
19. M. Meyer, M. Kircher, M.-T. Gansauge, H. Li, F. Racimo, S. Mallick, J. G. Schraiber, F. Jay, K. Prufer, C. de Filippo, P. H. Sudmant, C. Alkan, Q. Fu, R. Do, N. Rohland, A. Tandon, M. Siebauer, R. E. Green, K. Bryc, A. W. Briggs, U. Stenzel, J. Dabney, J. Shendure, J. Kitzman, M. F. Hammer, M. V. Shunkov, A. P. Derevianko, N. Patterson, A. M. Andrés, E. E. Eichler, M. Slatkin, D. Reich, J. Kelso, S. Pääbo, A high-coverage genome sequence from an archaic Denisovan individual. *Science* **338**, 222–226 (2012).
20. K. Prufer, C. de Filippo, S. Grote, F. Mafessoni, P. Korlević, M. Hajdinjak, B. Vernot, L. Skov, P. Hsieh, S. Peyrégne, D. Reher, C. Hopfe, S. Nagel, T. Maricic, Q. Fu, C. Theunert, R. Rogers, P. Skoglund, M. Chintalapati, M. Dannemann, B. J. Nelson, F. M. Key, P. Rudan, Ž. Kućan, I. Gušić, L. V. Golovanova, V. B. Doronichev, N. Patterson, D. Reich, E. E. Eichler, M. Slatkin, M. H. Schierup, A. M. Andrés, J. Kelso, M. Meyer, S. Pääbo, A high-coverage Neandertal genome from Vindija Cave in Croatia. *Science* **358**, 655–658 (2017).
21. Initial sequence of the chimpanzee genome and comparison with the human genome. *Nature* **437**, 69–87 (2005).
22. K. Prüfer, K. Munch, I. Hellmann, K. Akagi, J. R. Miller, B. Walenz, S. Koren, G. Sutton, C. Kodira, R. Winer, J. R. Knight, J. C. Mullikin, S. J. Meader, C. P. Ponting, G. Lunter, S. Higashino, A. Hobolth, J. Dutheil, E. Karakoç, C. Alkan, S. Sajjadian, C. R. Catacchio, M. Ventura, T. Marques-Bonet, E. E. Eichler, C. André, R. Atencia, L. Mugisha, J. Junhold, N. Patterson, M. Siebauer, J. M. Good, A. Fischer, S. E. Ptak, M. Lachmann, D. E. Symer, T. Mailund, M. H. Schierup, A. M. Andrés, J. Kelso, S. Pääbo, The bonobo genome compared with the chimpanzee and human genomes. *Nature* **486**, 527–531 (2012).
23. A. Scally, J. Y. Dutheil, L. W. Hillier, G. E. Jordan, I. Goodhead, J. Herrero, A. Hobolth, T. Lappalainen, T. Mailund, T. Marques-Bonet, S. McCarthy, S. H. Montgomery, P. C. Schwalie, Y. A. Tang, M. C. Ward, Y. Xue, B. Yngvadottir, C. Alkan, L. N. Andersen, Q. Ayub, E. V. Ball, K. Beal, B. J. Bradley, Y. Chen, C. M. Clee, S. Fitzgerald, T. A. Graves, Y. Gu, P. Heath, A. Heger, E. Karakoc, A. Kolb-Kokocinski, G. K. Laird, G. Lunter, S. Meader, M. Mort, J. C. Mullikin, K. Munch, T. D. O'Connor, A. D. Phillips, J. Prado-Martinez, A. S. Rogers, S. Sajjadian, D. Schmidt, K. Shaw, J. T. Simpson, P. D. Stenson, D. J. Turner, L. Vigilant, A. J. Vilella, W. Whitener, B. Zhu, D. N. Cooper, P. de Jong, E. T. Dermitzakis, E. E. Eichler, P. Flicek, N. Goldman, N. I. Mundy, Z. Ning, D. T. Odom, C. P. Ponting, M. A. Quail, O. A. Ryder, S. M. Searle, W. C. Warren, R. K. Wilson, M. H. Schierup, J. Rogers, C. Tyler-Smith, R. Durbin, Insights into hominid evolution from the gorilla genome sequence. *Nature* **483**, 169–175 (2012).
24. D. P. Locke, L. W. Hillier, W. C. Warren, K. C. Worley, L. V. Nazareth, D. M. Muzny, S. P. Yang, Z. Wang, A. T. Chinwalla, P. Minx, M. Mitreva, L. Cook, K. D. Delehaunty, C. Fronick, H. Schmidt, L. A. Fulton, R. S. Fulton, J. O. Nelson, V. Magrini, C. Pohl, T. A. Graves, C. Markovic, A. Cree, H. H. Dinh, J. Hume, C. L. Kovar, G. R. Fowler, G. Lunter, S. Meader, A. Heger, C. P. Ponting, T. Marques-Bonet, C. Alkan, L. Chen, Z. Cheng, J. M. Kidd, E. E. Eichler, S. White, S. Searle, A. J. Vilella, Y. Chen, P. Flicek, J. Ma, B. Raney, B. Suh, R. Burhans, J. Herrero, D. Haussler, R. Faria, O. Fernando, F. Darré, D. Farré, E. Gazave, M. Oliva, A. Navarro, R. Roberto, O. Capozzi, N. Archidiacono, G. D. Valle, S. Purgato, M. Rocchi, M. K. Konkel, J. A. Walker, B. Ullmer, M. A. Batzer, A. F. A. Smit, R. Hubley, C. Casola, D. R. Schrider, M. W. Hahn, V. Quesada, X. S. Puente, G. R. Ordoñez, C. López-Otín, T. Vinar, B. Brejova, A. Ratan, R. S. Harris, W. Miller, C. Kosiol, H. A. Lawson, V. Taliwal, A. L. Martins, A. Siepel, A. RoyChoudhury, X. Ma, J. Degenhardt, C. D. Bustamante, R. N. Gutenkunst, T. Mailund, J. Y. Dutheil, A. Hobolth, M. H. Schierup, O. A. Ryder, Y. Yoshinaga, P. J. de Jong, G. M. Weinstock, J. Rogers, E. R. Mardis, R. A. Gibbs, R. K. Wilson, Comparative and demographic analysis of orang-utan genomes. *Nature* **469**, 529–533 (2011).
25. P. Skoglund, A. Götherström, M. Jakobsson, Estimation of population divergence times from non-overlapping genomic sequences: Examples from dogs and wolves. *Mol. Biol. Evol.* **28**, 1505–1517 (2011).
26. J.-J. Hublin, W. Roebroeks, Ebb and flow or regional extinctions? On the character of Neandertal occupation of northern environments. *Comptes Rendus Palevol* **8**, 503–509 (2009).
27. W. Roebroeks, J.-J. Hublin, K. MacDonald, Continuities and discontinuities in Neandertal presence: A closer look at Northwestern Europe. *Dev. Quatern. Sci.* **14**, 113–123 (2011).
28. M. Kircher, S. Sawyer, M. Meyer, Double indexing overcomes inaccuracies in multiplex sequencing on the Illumina platform. *Nucleic Acids Res.* **40**, e3 (2012).
29. V. Slon, C. Hopfe, C. L. Weiß, F. Mafessoni, M. de la Rasilla, C. Lalueza-Fox, A. Rosas, M. Soressi, M. V. Knul, R. Miller, J. R. Stewart, A. P. Derevianko, Z. Jacobs, B. Li, R. G. Roberts, M. V. Shunkov, H. de Lumley, C. Perrenoud, I. Gušić, Ž. Kućan, P. Rudan, A. Aximu-Petri, E. Essel, S. Nagel, B. Nickel, A. Schmidt, K. Prüfer, J. Kelso, H. A. Burbano, S. Pääbo, M. Meyer, Neandertal and Denisovan DNA from Pleistocene sediments. *Science* **356**, 605–608 (2017).
30. R. M. Andrews, I. Kubacka, P. F. Chinnery, R. N. Lightowlers, D. M. Turnbull, N. Howell, Reanalysis and revision of the Cambridge reference sequence for human mitochondrial DNA. *Nat. Genet.* **23**, 147 (1999).
31. M. L. Speir, A. S. Zweig, K. R. Rosenbloom, B. J. Raney, B. Paten, P. Nejad, B. T. Lee, K. Learned, D. Karolchik, A. S. Hinrichs, S. Heitner, R. A. Harte, M. Haeussler, L. Guruvadoo, P. A. Fujita, C. Eisenhart, M. Diekhans, H. Clawson, J. Casper, G. P. Barber, D. Haussler, R. M. Kuhn, W. J. Kent, The UCSC Genome Browser database: 2016 update. *Nucleic Acids Res.* **44**, D717–D725 (2016).
32. P. R. Staab, S. Zhu, D. Metzler, G. Lunter, scrm: Efficiently simulating long sequences using the approximated coalescent with recombination. *Bioinformatics* **31**, 1680–1682 (2015).
33. H. Li, R. Durbin, Inference of human population history from individual whole-genome sequences. *Nature* **475**, 493–496 (2011).
34. R. E. Green, J. Krause, A. W. Briggs, T. Maricic, U. Stenzel, M. Kircher, N. Patterson, H. Li, W. Zhai, M. H.-Y. Fritz, N. F. Hansen, E. Y. Durand, A. S. Malaspinas, J. D. Jensen, T. Marques-Bonet, C. Alkan, K. Prüfer, M. Meyer, H. A. Burbano, J. M. Good, R. Schultz, A. Aximu-Petri, A. Butthof, B. Höber, B. Höffner, M. Siegemund, A. Weihmann, C. Nusbaum, E. S. Lander, C. Russ, N. Novod, J. Affourtit, M. Egholm, C. Verna, P. Rudan, D. Brajkovic, Z. Kucan, I. Gušic, V. B. Doronichev, L. V. Golovanova, C. Lalueza-Fox, M. de la Rasilla, J. Fortea, A. Rosas, R. W. Schmitz, P. L. F. Johnson, E. E. Eichler, D. Falush, E. Birney, J. C. Mullikin, M. Slatkin, R. Nielsen, J. Kelso, M. Lachmann, D. Reich, S. Pääbo, A draft sequence of the Neandertal genome. *Science* **328**, 710–722 (2010).

35. S. Castellano, G. Parra, F. A. Sánchez-Quinto, F. Racimo, M. Kuhlwilm, M. Kircher, S. Sawyer, Q. Fu, A. Heinze, B. Nickel, J. Dabney, M. Siebauer, L. White, H. A. Burbano, G. Renaud, U. Stenzel, C. Lalueza-Fox, M. de la Rasilla, A. Rosas, P. Rudan, D. Brajkovi, Ž. Kucan, I. Gušic, M. V. Shunkov, A. P. Derevianko, B. Viola, M. Meyer, J. Kelso, A. M. Andres, S. Pääbo, Patterns of coding variation in the complete exomes of three Neandertals. *Proc. Natl. Acad. Sci. U. S. A.* **111**, 6666–6671 (2014).
36. M. Kuhlwilm, I. Gronau, M. J. Hubisz, C. de Filippo, J. Prado-Martinez, M. Kircher, Q. Fu, H. A. Burbano, C. Lalueza-Fox, M. de la Rasilla, A. Rosas, P. Rudan, D. Brajkovic, Ž. Kucan, I. Gušic, T. Marques-Bonet, A. M. Andrés, B. Viola, S. Pääbo, M. Meyer, A. Siepel, S. Castellano, Ancient gene flow from early modern humans into Eastern Neanderthals. *Nature* **530**, 429–433 (2016).
37. L. E. Lisiecki, M. E. Raymo, A Pliocene-Pleistocene stack of 57 globally distributed benthic $\delta^{18}O$ records. *Paleoceanography* **20**, PA1003 (2005).
38. L. Orlando, A. Ginolhac, M. Raghavan, J. Vilstrup, M. Rasmussen, K. Magnussen, K. E. Steinmann, P. Kapranov, J. F. Thompson, G. Zazula, D. Froese, I. Moltke, B. Shapiro, M. Hofreiter, K. A. S. Al-Rasheid, M. T. P. Gilbert, E. Willerslev, True single-molecule DNA sequencing of a pleistocene horse bone. *Genome Res.* **21**, 1705–1719 (2011).
39. P. B. Damgaard, A. Margaryan, H. Schroeder, L. Orlando, E. Willerslev, M. E. Allentoft, Improving access to endogenous DNA in ancient bones and teeth. *Sci. Rep.* **5**, 11184 (2015).
40. I. Glocke, M. Meyer, Extending the spectrum of DNA sequences retrieved from ancient bones and teeth. *Genome Res.* **27**, 1230–1237 (2017).
41. V. Slon, I. Glocke, R. Barkai, A. Gopher, I. Hershkovitz, M. Meyer, Mammalian mitochondrial capture, a tool for rapid screening of DNA preservation in faunal and undiagnostic remains, and its application to Middle Pleistocene specimens from Qesem Cave (Israel). *Quatern. Int.* **398**, 210–218 (2016).
42. J. Dabney, M. Meyer, Length and GC-biases during sequencing library amplification: A comparison of various polymerase-buffer systems with ancient and modern DNA sequencing libraries. *Biotechniques* **52**, 87–94 (2012).
43. M. M. DeAngelis, D. G. Wang, T. L. Hawkins, Solid-phase reversible immobilization for the isolation of PCR products. *Nucleic Acids Res.* **23**, 4742–4743 (1995).
44. T. Maricic, M. Whitten, S. Pääbo, Multiplexed DNA sequence capture of mitochondrial genomes using PCR products. *PLOS ONE* **5**, e14004 (2010).
45. Q. Fu, M. Meyer, X. Gao, U. Stenzel, H. A. Burbano, J. Kelso, S. Pääbo, DNA analysis of an early modern human from Tianyuan Cave, China. *Proc. Natl. Acad. Sci. U. S. A.* **110**, 2223–2227 (2013).
46. M. Meyer, M. Kircher, Illumina sequencing library preparation for highly multiplexed target capture and sequencing. *Cold Spring Harb. Protoc.* **2010**, pdb. prot5448 (2010).
47. D. R. Bentley, S. Balasubramanian, H. P. Swerdlow, G. P. Smith, J. Milton, C. G. Brown, K. P. Hall, D. J. Evers, C. L. Barnes, H. R. Bignell, J. M. Boutell, J. Bryant, R. J. Carter, R. Keira Cheetham, A. J. Cox, D. J. Ellis, M. R. Flatbush, N. A. Gormley, S. J. Humphray, L. J. Irving, M. S. Karbelashvili, S. M. Kirk, H. Li, X. Liu, K. S. Maisinger, L. J. Murray, B. Obradovic, T. Ost, M. L. Parkinson, M. R. Pratt, I. M. J. Rasolonjatovo, M. T. Reed, R. Rigatti, C. Rodighiero, M. T. Ross, A. Sabot, S. V. Sankar, A. Scally, G. P. Schroth, M. E. Smith, V. P. Smith, A. Spiridou, P. E. Torrance, S. S. Tzonev, E. H. Vermaas, K. Walter, X. Wu, L. Zhang, M. D. Alam, C. Anastasi, I. C. Aniebo, D. M. D. Bailey, I. R. Bancarz, S. Banerjee, S. G. Barbour, P. A. Baybayan, V. A. Benoit, K. F. Benson, C. Bevis, P. J. Black, A. Boodhun, J. S. Brennan, J. A. Bridgham, R. C. Brown, A. A. Brown, D. H. Buermann, A. A. Bundu, J. C. Burrows, N. P. Carter, N. Castillo, M. Chiara E. Catenazzi, S. Chang, R. Neil Cooley, N. R. Crake, O. O. Dada, K. D. Diakoumakos, B. Dominguez-Fernandez, D. J. Earnshaw, U. C. Egbujor, D. W. Elmore, S. S. Etchin, M. R. Ewan, M. Fedurco, L. J. Fraser, K. V. Fuentes Fajardo, W. Scott Furey, D. George, K. J. Gietzen, C. P. Goddard, G. S. Golda, P. A. Granieri, D. E. Green, D. L. Gustafson, N. F. Hansen, K. Harnish, C. D. Haudenschild, N. I. Heyer, M. M. Hims, J. T. Ho, A. M. Horgan, K. Hoschler, S. Hurwitz, D. V. Ivanov, M. Q. Johnson, T. James, T. A. Huw Jones, G.-D. Kang, T. H. Kerelska, A. D. Kersey, I. Khrebtukova, A. P. Kindwall, Z. Kingsbury, P. I. Kokko-Gonzales, A. Kumar, M. A. Laurent, C. T. Lawley, S. E. Lee, X. Lee, A. K. Liao, J. A. Loch, M. Lok, S. Luo, R. M. Mammen, J. W. Martin, P. G. McCauley, P. McNitt, P. Mehta, K. W. Moon, J. W. Mullens, T. Newington, Z. Ning, B. Ling Ng, S. M. Novo, M. J. O'Neill, M. A. Osborne, A. Osnowski, O. Ostadan, L. L. Paraschos, L. Pickering, A. C. Pike, A. C. Pike, D. Chris Pinkard, D. P. Pliskin, J. Podhasky, V. J. Quijano, C. Raczy, V. H. Rae, S. R. Rawlings, A. Chiva Rodriguez, P. M. Roe, J. Rogers, M. C. Rogert Bacigalupo, N. Romanov, A. Romieu, R. K. Roth, N. J. Rourke, S. T. Ruediger, E. Rusman, R. M. Sanches-Kuiper, M. R. Schenker, J. M. Seoane, R. J. Shaw, M. K. Shiver, S. W. Short, N. L. Sizto, J. P. Sluis, M. A. Smith, J. Ernest Sohna Sohna, E. J. Spence, K. Stevens, N. Sutton, L. Szajkowski, C. L. Tregidgo, G. Turcatti, S. vandeVondele, Y. Verhovsky, S. M. Virk, S. Wakelin, G. C. Walcott, J. Wang, G. J. Worsley, J. Yan, L. Yau, M. Zuerlein, J. Rogers, J. C. Mullikin, M. E. Hurles, N. J. McCooke, J. S. West, F. L. Oaks, P. L. Lundberg, D. Klenerman, R. Durbin, A. J. Smith, Accurate whole human genome sequencing using reversible terminator chemistry. *Nature* **456**, 53–59 (2008).
48. G. Renaud, U. Stenzel, J. Kelso, leeHom: Adaptor trimming and merging for Illumina sequencing reads. *Nucleic Acids Res.* **42**, e141 (2014).
49. H. Li, R. Durbin, Fast and accurate long-read alignment with Burrows-Wheeler transform. *Bioinformatics* **26**, 589–595 (2010).
50. C. de Filippo, M. Meyer, K. Prüfer, Quantifying and reducing spurious alignments for the analysis of ultra-short ancient DNA sequences. *BMC Biol.* **16**, 121 (2018).
51. H. Li, A statistical framework for SNP calling, mutation discovery, association mapping and population genetical parameter estimation from sequencing data. *Bioinformatics* **27**, 2987–2993 (2011).
52. T. M. Smith, M. Toussaint, D. J. Reid, A. J. Olejniczak, J.-J. Hublin, Rapid dental development in a Middle Paleolithic Belgian Neanderthal. *Proc. Natl. Acad. Sci. U. S. A.* **104**, 20220–20225 (2007).
53. C. E. Oxnard, *Fossils,Teeth, and Sex: New Perspectives on Human Evolution* (University of Washington Press, 1987).
54. S. M. Garn, W. L. Van Alstine Jr., P. E. Cole, Intraindividual root-length correlations. *J. Dent. Res.* **57**, 270 (1978).
55. S. M. Garn, P. E. Cole, W. L. Van Alstine, Sex discriminatory effectiveness using combinations of root lengths and crown diameters. *Am. J. Phys. Anthropol.* **50**, 115–117 (1979).
56. R. Jakobsson, V. Lind, Variation in root length of the permanent maxillary central incisor. *Scand. J. Dent. Res.* **81**, 335–338 (1973).
57. R. Lähdesmäki, *Sex Chromosomes in Human Tooth Root Growth: Radiographic Studies on 47, XYY Males, 46, XY Females, 47, XXY Males and 45, X/46, XX Females* (University of Oulu, 2006).
58. R. Lähdesmäki, L. Alvesalo, Root lengths in the permanent teeth of Klinefelter (47,XXY) men. *Arch. Oral Biol.* **52**, 822–827 (2007).
59. L. Alvesalo, E. Tammisalo, G. Townsend, Upper central incisor and canine tooth crown size in 47,XXY males. *J. Dent. Res.* **70**, 1057–1060 (1991).
60. G. T. Schwartz, M. C. Dean, Sexual dimorphism in modern human permanent teeth. *Am. J. Phys. Anthropol.* **128**, 312–317 (2005).
61. U. Zilberman, P. Smith, Sex- and age-related differences in primary and secondary dentin formation. *Adv. Dent. Res.* **15**, 42–45 (2001).
62. S. R. Loth, M. Henneberg, Ramus flexure and symphyseal base shape: Sexually dimorphic morphology in the premodern hominid mandible. *Am. J. Phys. Anthropol.* **1997**, 157–158 (1997).
63. R. E. Green, A.-S. Malaspinas, J. Krause, A. W. Briggs, P. L. F. Johnson, C. Uhler, M. Meyer, J. M. Good, T. Maricic, U. Stenzel, K. Prüfer, M. Siebauer, H. A. Burbano, M. Ronan, J. M. Rothberg, M. Egholm, P. Rudan, D. Brajković, Ž. Kućan, I. Gušić, M. Wikström, L. Laakkonen, J. Kelso, M. Slatkin, S. Pääbo, A complete Neandertal mitochondrial genome sequence determined by high-throughput sequencing. *Cell* **134**, 416–426 (2008).
64. K. Katoh, D. M. Standley, MAFFT multiple sequence alignment software version 7: Improvements in performance and usability. *Mol. Biol. Evol.* **30**, 772–780 (2013).
65. H. Rougier, I. Crevecoeur, C. Beauval, C. Posth, D. Flas, C. Wißing, A. Furtwängler, M. Germonpré, A. Gómez-Olivencia, P. Semal, J. van der Plicht, H. Bocherens, J. Krause, Neandertal cannibalism and Neandertal bones used as tools in Northern Europe. *Sci. Rep.* **6**, 29005 (2016).
66. A. W. Briggs, J. M. Good, R. E. Green, J. Krause, T. Maricic, U. Stenzel, C. Lalueza-Fox, P. Rudan, D. Brajković, Ž. Kucan, I. Gušić, R. Schmitz, V. B. Doronichev, L. V. Golovanova, M. de la Rasilla, J. Fortea, A. Rosas, S. Pääbo, Targeted retrieval and analysis of five Neandertal mtDNA genomes. *Science* **325**, 318–321 (2009).
67. P. Skoglund, B. H. Northoff, M. V. Shunkov, A. P. Derevianko, S. Pääbo, J. Krause, M. Jakobsson, Separating endogenous ancient DNA from modern day contamination in a Siberian Neandertal. *Proc. Natl. Acad. Sci. U. S. A.* **111**, 2229–2234 (2014).
68. S. Brown, T. Higham, V. Slon, S. Pääbo, M. Meyer, K. Douka, F. Brock, D. Comeskey, N. Procopio, M. Shunkov, A. Derevianko, M. Buckley, Identification of a new hominin bone from Denisova Cave, Siberia using collagen fingerprinting and mitochondrial DNA analysis. *Sci. Rep.* **6**, 23559 (2016).
69. M.-T. Gansauge, M. Meyer, Selective enrichment of damaged DNA molecules for ancient genome sequencing. *Genome Res.* **24**, 1543–1549 (2014).
70. L. Ermini, C. Olivieri, E. Rizzi, G. Corti, R. Bonnal, P. Soares, S. Luciani, I. Marota, G. De Bellis, M. B. Richards, F. Rollo, Complete mitochondrial genome sequence of the Tyrolean Iceman. *Curr. Biol.* **18**, 1687–1693 (2008).
71. M. T. P. Gilbert, T. Kivisild, B. Grønnow, P. K. Andersen, E. Metspalu, M. Reidla, E. Tamm, E. Axelsson, A. Götherström, P. F. Campos, M. Rasmussen, M. Metspalu, T. F. G. Higham, J.-L. Schwenninger, R. Nathan, C.-J. De Hoog, A. Koch, L. N. Møller, C. Andreasen, M. Meldgaard, R. Villems, C. Bendixen, E. Willerslev, Paleo-Eskimo mtDNA genome reveals matrilineal discontinuity in Greenland. *Science* **320**, 1787–1789 (2008).
72. J. Krause, A. W. Briggs, M. Kircher, T. Maricic, N. Zwyns, A. Derevianko, S. Pääbo, A complete mtDNA genome of an early modern human from Kostenki, Russia. *Curr. Biol.* **20**, 231–236 (2010).
73. Q. Fu, A. Mittnik, P. L. F. Johnson, K. Bos, M. Lari, R. Bollongino, C. Sun, L. Giemsch, R. Schmitz, J. Burger, A. M. Ronchitelli, F. Martini, R. G. Cremonesi, J. Svoboda, P. Bauer,

D. Caramelli, S. Castellano, D. Reich, S. Pääbo, J. Krause, A revised timescale for human evolution based on ancient mitochondrial genomes. *Curr. Biol.* **23**, 553–559 (2013).
74. Q. Fu, H. Li, P. Moorjani, F. Jay, S. M. Slepchenko, A. A. Bondarev, P. L. F. Johnson, A. Aximu-Petri, K. Prüfer, C. de Filippo, M. Meyer, N. Zwyns, D. C. Salazar-García, Y. V. Kuzmin, S. G. Keates, P. A. Kosintsev, D. I. Razhev, M. P. Richards, N. V. Peristov, M. Lachmann, K. Douka, T. F. G. Higham, M. Slatkin, J.-J. Hublin, D. Reich, J. Kelso, T. B. Viola, S. Pääbo, Genome sequence of a 45,000-year-old modern human from western Siberia. *Nature* **514**, 445–449 (2014).
75. S. Sawyer, G. Renaud, B. Viola, J.-J. Hublin, M.-T. Gansauge, M. V. Shunkov, A. P. Derevianko, K. Prüfer, J. Kelso, S. Pääbo, Nuclear and mitochondrial DNA sequences from two Denisovan individuals. *Proc. Natl. Acad. Sci. U. S. A.* **112**, 15696–15700 (2015).
76. V. Slon, B. Viola, G. Renaud, M.-T. Gansauge, S. Benazzi, S. Sawyer, J.-J. Hublin, M. V. Shunkov, A. P. Derevianko, J. Kelso, K. Prüfer, M. Meyer, S. Pääbo, A fourth Denisovan individual. *Sci. Adv.* **3**, e1700186 (2017).
77. J. Krause, Q. Fu, J. M. Good, B. Viola, M. V. Shunkov, A. P. Derevianko, S. Pääbo, The complete mitochondrial DNA genome of an unknown hominin from southern Siberia. *Nature* **464**, 894–897 (2010).
78. M. Meyer, Q. Fu, A. Aximu-Petri, I. Glocke, B. Nickel, J.-L. Arsuaga, I. Martínez, A. Gracia, J. M. B. de Castro, E. Carbonell, S. Pääbo, A mitochondrial genome sequence of a hominin from Sima de los Huesos. *Nature* **505**, 403–406 (2014).
79. U. Arnason, X. Xu, A. Gullberg, Comparison between the complete mitochondrial DNA sequences of *Homo* and the common chimpanzee based on nonchimeric sequences. *J. Mol. Evol.* **42**, 145–152 (1996).
80. M. Nei, S. Kumar, *Molecular Evolution and Phylogenetics* (Oxford Univ. Press, 2000).
81. K. Tamura, G. Stecher, D. Peterson, A. Filipski, S. Kumar, MEGA6: Molecular Evolutionary Genetics Analysis version 6. 0. *Mol. Biol. Evol.* **30**, 2725–2729 (2013).
82. R. Bouckaert, J. Heled, D. Kühnert, T. Vaughan, C.-H. Wu, D. Xie, M. A. Suchard, A. Rambaut, A. J. Drummond, BEAST 2: A software platform for Bayesian evolutionary analysis. *PLOS Comput. Biol.* **10**, e1003537 (2014).
83. S. Pirson, M. Toussaint, D. Bonjean, K. Di Modica, in *Landscapes and Landforms of Belgium and Luxembourg*, A. Demoulin, Ed. (Springer International Publishing, 2018), pp. 357–383.
84. K. Tamura, M. Nei, Estimation of the number of nucleotide substitutions in the control region of mitochondrial DNA in humans and chimpanzees. *Mol. Biol. Evol.* **10**, 512–526 (1993).
85. J. M. Santorum, D. Darriba, G. L. Taboada, D. Posada, jmodeltest.org: Selection of nucleotide substitution models on the cloud. *Bioinformatics* **30**, 1310–1311 (2014).
86. R. E. Wood, T. F. G. Higham, T. De Torres, N. Tisnérat-Laborde, H. Valladas, J. E. Ortiz, C. Lalueza-Fox, S. Sánchez-Moral, J. C. Cañaveras, A. Rosas, D. Santamaría, M. de la Rasilla, A new date for the Neanderthals from El Sidrón Cave (Asturias, northern Spain). *Archaeometry* **55**, 148–158 (2013).
87. S. Sawyer, J. Krause, K. Guschanski, V. Savolainen, S. Pääbo, Temporal patterns of nucleotide misincorporations and DNA fragmentation in ancient DNA. *PLOS ONE* **7**, e34131 (2012).
88. J. Dabney, M. Meyer, S. Pääbo, Ancient DNA damage. *Cold Spring Harb. Perspect. Biol.* **5**, a012567 (2013).
89. The 1000 Genomes ProjectConsortium, A global reference for human genetic variation. *Nature* **526**, 68–74 (2015).
90. M. G. Ross, C. Russ, M. Costello, A. Hollinger, N. J. Lennon, R. Hegarty, C. Nusbaum, D. B. Jaffe, Characterizing and measuring bias in sequence data. *Genome Biol.* **14**, R51 (2013).
91. T. C. Glenn, Field guide to next-generation DNA sequencers. *Mol. Ecol. Resour.* **11**, 759–769 (2011).
92. M. Schubert, A. Ginolhac, S. Lindgreen, J. F. Thompson, K. A. S. Al-Rasheid, E. Willerslev, A. Krogh, L. Orlando, Improving ancient DNA read mapping against modern reference genomes. *BMC Genomics* **13**, 178 (2012).
93. G. Lunter, M. Goodson, Stampy: A statistical algorithm for sensitive and fast mapping of Illumina sequence reads. *Genome Res.* **21**, 936–939 (2011).
94. J. Wakeley, *Coalescent Theory: An Introduction* (Macmillan Learning, 2016).
95. R. R. Hudson, Testing the constant-rate neutral allele model with protein sequence data. *Evolution* **37**, 203–217 (1983).
96. N. Takahata, Gene genealogy in three related populations: Consistency probability between gene and population trees. *Genetics* **122**, 957–966 (1989).
97. N. A. Rosenberg, The probability of topological concordance of gene trees and species trees. *Theor. Popul. Biol.* **61**, 225–247 (2002).
98. R. R. Hudson, Generating samples under a Wright-Fisher neutral model of genetic variation. *Bioinformatics* **18**, 337–338 (2002).
99. A. Scally, R. Durbin, Revising the human mutation rate: Implications for understanding human evolution. *Nat. Rev. Genet.* **13**, 745–753 (2012).
100. H. Chen, The joint allele frequency spectrum of multiple populations: A coalescent theory approach. *Theor. Popul. Biol.* **81**, 179–195 (2012).
101. S. Tavaré, Line-of-descent and genealogical processes, and their applications in population genetics models. *Theor. Popul. Biol.* **26**, 119–164 (1984).
102. B. Herrmann, The postcranial remains of the Neanderthalman from Le Moustier. *Z. Morphol. Anthropol.* **68**, 129–149 (1977).
103. V. Volpato, R. Macchiarelli, D. Guatelli-Steinberg, I. Fiore, L. Bondioli, D. W. Frayer, Hand to mouth in a Neandertal: Right-handedness in Regourdou 1. *PLOS ONE* **7**, e43949 (2012).
104. E. Trinkaus, S. E. Churchill, C. B. Ruff, B. Vandermeersch, Long bone shaft robusticity and body proportions of the Saint-Césaire 1 Châtelperronian Neanderthal. *J. Archaeol. Sci.* **26**, 753–773 (1999).
105. Y. Rak, B. Arensburg, Kebara 2 Neanderthal pelvis: First look at a complete inlet. *Am. J. Phys. Anthropol.* **73**, 227–231 (1987).
106. H. Suzuki, F. Takai, *The Amud Man and His Cave Site* (Academic Press of Japan, 1970).
107. S. Condemi, *Les néandertaliens de La Chaise: Abri Bourgeois-Delaunay* (Comité de travaux historiques et scientifiques, 2001).
108. A. Thoma, Were the Spy fossils evolutionary intermediates between Classic Neandertal and Modern Man? *J. Hum. Evol.* **4**, 387–400 (1975).
109. E. Trinkaus, Sexual differences in Neanderthal limb bones. *J. Hum. Evol.* **9**, 377–397 (1980).
110. H. Klaatsch, O. Hauser, Homo aurignacensis Hauseri: Ein paläolithischer Skelettfund aus dem unteren Aurignacien der Station Combe-Capelle bei Montferrand (Périgord) *Praehistorische Zeitschrift*, **1**, 273–338 (1910).
111. P. Mahoney, Human dental microwear from Ohalo II (22,500-23,500 cal BP), southern Levant. *Am. J. Phys. Anthropol.* **132**, 489–500 (2007).
112. I. Hershkovitz, M. S. Speirs, D. Frayer, D. Nadel, S. Wish-Baratz, B. Arensburg, Ohalo II H2: A 19,000-year-old skeleton from a water-logged site at the Sea of Galilee, Israel. *Am. J. Phys. Anthropol.* **96**, 215–234 (1995).
113. W. Henke, Die magdalénienzeitlichen Menschenfunde von Oberkassel bei Bonn. *Bonner Jahrbücher* **186**, 317–366 (1986).
114. A. Le Cabec, P. Gunz, K. Kupczik, J. Braga, J.-J. Hublin, Anterior tooth root morphology and size in Neanderthals: Taxonomic and functional implications. *J. Hum. Evol.* **64**, 169–193 (2013).

Acknowledgments: We thank B. Schellbach and A. Weihmann for DNA sequencing; I. Bünger and R. Schultz for their technical support; A. Huebner and E. Macholdt for their assistance with the BEAST analyses; B. Evans, T. Lauer, A. Schuh, and B. Vernot for helpful discussion; and B. M. Peter, P. Skoglund, and M. Slatkin for both helpful discussion and comments on the manuscript. **Funding:** This study was funded by the Max Planck Society and the European Research Council (grant agreement number 694707 to S.Pa.). **Author contributions:** S.Pe., J.Ke., M.M., S.Pa., and K.P. designed the research. V.S., M.H., S.N., B.N., and E.E. performed the laboratory work. K.W., N.J.C., C.J.K., C.P., J.Kr., G.A., D.B., K.D.M., and M.T. provided ancient samples. S.Pe., V.S., F.M., and C.d.F. analyzed genetic data. A.L.C. and M.T. analyzed morphologic data. S.Pe. and K.P. wrote the paper, with input from all authors. **Competing interests:** The authors declare that they have no competing interests. **Data and materials availability:** Sequencing data generated in this study are deposited in http://cdna.eva.mpg.de/neandertal and the European Nucleotide Archive (PRJEB29475). The mitochondrial sequence of *Scladina* is available in GenBank (MK123269). The mitochondrial sequence of *HST* has been updated in GenBank (KY751400.2). All data needed to evaluate the conclusions in the paper are present in the paper and/or the Supplementary Materials. Additional data related to this paper may be requested from the authors.

Submitted 7 January 2019
Accepted 22 May 2019
Published 26 June 2019
10.1126/sciadv.aaw5873

Citation: S. Peyrégne, V. Slon, F. Mafessoni, C. de Filippo, M. Hajdinjak, S. Nagel, B. Nickel, E. Essel, A. Le Cabec, K. Wehrberger, N. J. Conard, C. J. Kind, C. Posth, J. Krause, G. Abrams, D. Bonjean, K. Di Modica, M. Toussaint, J. Kelso, M. Meyer, S. Pääbo, K. Prüfer, Nuclear DNA from two early Neandertals reveals 80,000 years of genetic continuity in Europe. *Sci. Adv.* **5**, eaaw5873 (2019).

ScienceAdvances

Nuclear DNA from two early Neandertals reveals 80,000 years of genetic continuity in Europe

Stéphane Peyrégne, Viviane Slon, Fabrizio Mafessoni, Cesare de Filippo, Mateja Hajdinjak, Sarah Nagel, Birgit Nickel, Elena Essel, Adeline Le Cabec, Kurt Wehrberger, Nicholas J. Conard, Claus Joachim Kind, Cosimo Posth, Johannes Krause, Grégory Abrams, Dominique Bonjean, Kévin Di Modica, Michel Toussaint, Janet Kelso, Matthias Meyer, Svante Pääbo and Kay Prüfer

Sci Adv **5** (6), eaaw5873.
DOI: 10.1126/sciadv.aaw5873